Posted: May 22, 2020

Introducing Design Space-Independence in Beam Cross-Section Optimization

Chander Sen[1] and Jitendra Prasad[1]

[1]Department of Mechanical Engineering, Indian Institute of Technology Ropar, India
ORCID: 0000-0003-4274-1192,0000-0001-6389-955X
[*]Corresponding author: jprasad@iitrpr.ac.in

Abstract

The cross-sectional topology optimization of a slender load carrying member such as a beam typically begins with the choice of design space which is generally either a square or a rectangle. However, when subjected to bending and torsional loads, such design space may often lead to biased topologies as the material distribution is directed towards the boundaries. As it may be difficult to avoid square/rectangular design space, this work introduces a constraint which may help in decreasing the dependency on the shape of the design space. The constraint is on polar first moment of area and is different from the traditional weight constraint in a way that it simultaneously constrains the weight and enclosed volume. The outcomes from the new scheme are compared with those obtained through conventional compliance- and weight- based topology optimization formulation.

1 Introduction

Cross-section selection is one of the primary considerations in design of load carrying members such as beams, rods and shaft. Standard cross-section shapes such as I-beam, H-beam, box and circular sections are common choices of cross-sections which are easily available in different dimensions. However, finalizing the dimensions for different loading and failure criteria is an important task. In current times, the task is typically performed through topology optimization (Zuberi et al. (2010); Yiru et al. (2015); Vatanabe et al. (2016); Zhou et al. (2002); Patel et al. (2009); Kim and Kim (2000)). Kim and Kim (2000) used the technique for the first time in optimization of a beam cross-section, where, bending and torsional rigidities of the section were maximized for a prescribed material constraint. However, it was the work of Zhou et al. (2002) which simplified the cross-section optimization process using a compliance-weight based formulation under realistic modelling and loading conditions. In fact, the work introduced extrusion manufacturing constraint which could also be used for the cross-section optimization. Most of the later works on beam optimization were inspired from the same extrusion constraint formulation (Patel et al. (2009); Vatanabe et al. (2016)). To effectively demonstrate the efficacy of extrusion constraint, Zuberi et al. (2010) used different load combinations and design space geometries for yielding the optimal cross-sections. After this work, the focus on beam optimization algorithms relatively decreased until composite material beams became the topic of interest (Ren et al. (2016); Yiru et al. (2015); Blasques and Stolpe (2012)). In such beams, apart from weight, the fibre orientation is also optimized simultaneously. However, there are some limitations of the existing cross-section topology optimization formulations (i.e., compliance minimization against a weight constraint subject to an extrusion constraint). Firstly, the final topologies are primarily governed by the direction of load which increases the moment of inertia about a particular axis whereas neglecting the other. This consideration is particularly important in cases such as selection of the web thickness in an I-section, as compliance-weight based topology optimization would result in a thinner web and thick flanges for unidirectional vertical loading Patel et al. (2009). Therefore, it is obvious that the thin web could either fail due to shear or buckling. In that case, cross-section optimization will have no meaning if web thickness would require a re-calculation. Secondly, the final topologies depend upon the choice of initial design space. For example, for same value of weight constraint, beam subjected to vertical loads yield different final topologies for square and rectangular design spaces Zuberi et al. (2010). Therefore, the current work proposes a topology optimization scheme which besides generating robust cross-sections (i.e. resistance to tension, compression, shear and warping), could also decrease the effect of design space on the final cross-sections. Thirdly, the weight constrain in the conventional topology optimization constraints the total weight and not the enclosed volume, the resulting design may not be space-efficient. To address the aforementioned issues, this work suggests an alternative to weight constraint where the weight constraint is replaced by a constraint on polar first moment of area which simultaneously constrains both weight and space. As such, for a prescribed constraint value, the new scheme can generate different geometries for different weight. The scheme is tested for optimizing the cross-section of a prismatic cantilever beam under different loading conditions. Geometry of beam is represented by two-dimensional tiling of 16-noded hexahedral (brick) elements, where linear interpolation functions have been used along the cross-section (i.e. in transverse directions of the beam) and cubic interpolation functions have been used along the beam length (Fig. 1(a)). Such discretisation avoids the need for an extrusion constraint. The hybrid finite element model is first tested against a fully discretised model in terms of stress distribution at fixed end when subjected to a vertical end load. Subsequently, the newly developed topology optimization scheme is applied to optimize the cross-sections for different end loading conditions. The results are compared with those obtained using the conventional compliance-weight based topology optimization formulation. Further, the ability of the new scheme to generate design space independent topologies is tested which could carve circular and elliptical sections out of square design space when the beam is subjected to biaxial bending loads. Organization of rest of this paper is as follows. Section 2 describes the methodologies used for finite element modeling and topology optimization. The results have been presented in Section 3. Conclusions are given in Section 4, along with discussions and scope of future work.

2 Methodologies

2.1 Finite element model

As mentioned in Section 1, the finite element model uses a hybrid 16-noded element which spans across the beam length. The idea for the element is derived from Euler-Bernoulli Beam Theory (Popov (1968)). For any load F applied on the free end of a cantilever beam:

$$M = F.x = EI\frac{d^2u_y}{dx^2} \tag{1}$$

where u_y is the transverse deflection and M is the bending moment at a distance x from the free end, E is material stiffness and I is area moment of inertia. Hence, the transverse displacement u_y should at least be a cubic function of distance x. Accordingly, a cubic interpolation function is chosen along the length of the element. To keep the computational cost minimum, transverse interpolation functions are kept linear as accuracy in this direction can be taken care of by fine discretization. The shape functions for the element are accordingly derived and element stiffness matrix was computed by applying standard methods (Reddy (1993); Bathe (2006)). A standard beam model used by Liu et al. (2008) is discretized using the 16-noded elements (as discussed in detail in Section 3). The computational work has been done using an in-house code written in MATLAB® (Mathworks Inc., Boston). The finite element model developed here is then tested for a vertical end-loading case (Fig. 1(a)) against a fully discretised beam model developed and analysed in a commercial finite element analysis software (viz., ANSYS). The stress distribution at the fixed ends in both beams was found to be similar and nearly equal in magnitude (error in maximum stress within 10% , disregarding stress concentration at corners), as shown in Figs. 1(c) and (d).

2.2 Optimization problems

The conventional compliance-weight based topology optimization is first discussed. Thereafter, the compliance-polar first moment of area based topology optimization is introduced.

2.2.1 Minimization of compliance subject to weight constraint

The objective of this problem is to minimize structural compliance subject to a weight constraint, as in Sigmund (Sigmund 2001). The method used for structural topology optimization has been adapted from Andreassen et al. (2011). The basic optimization problem is given by:

$$\min\ c(x) = \mathbf{U}^T\mathbf{K}\mathbf{U} = \sum_{e=1}^{N}(x_e)^p u_e^T k_0 u_e \tag{2}$$

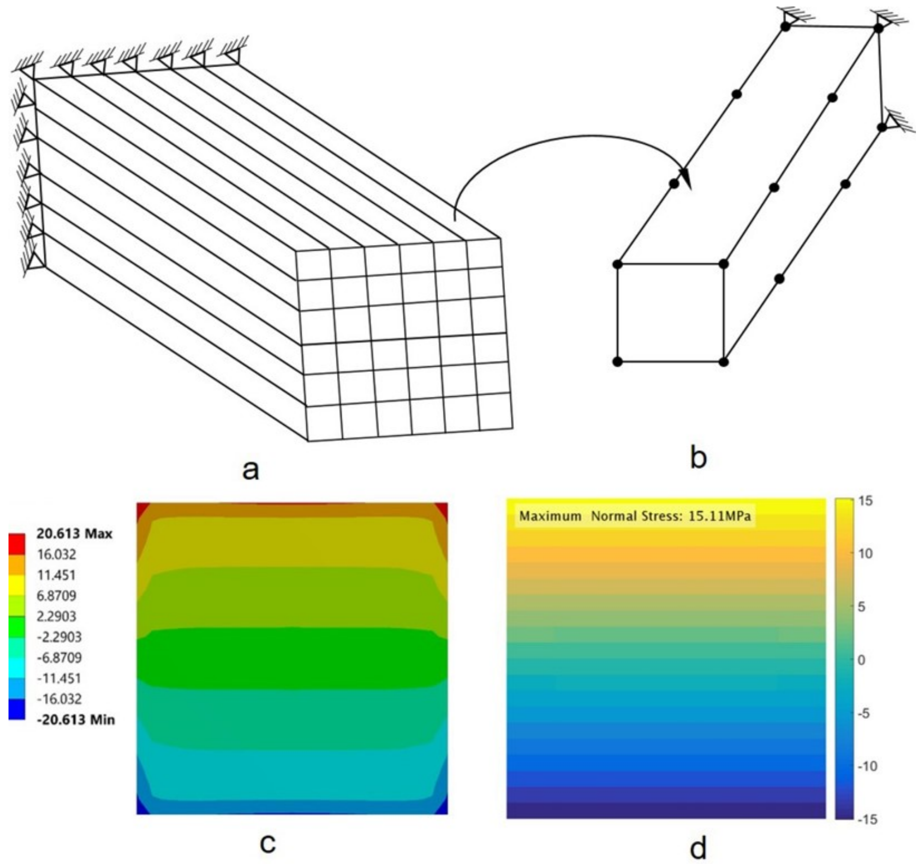

Figure 1: Geometry representation of a beam using 16-noded brick elements. (a) Beam discretization (for illustration only, actual discretization is generally 150×150 elements), (b) the 16-noded brick element; comparison of normal stress distribution at the fixed end of cantilever beam for a vertical load at the top edge of free end using a fully discretised (20×20×251 elements) finite element model analysed in ANSYS (c), and (d) the current modelling approach (20×20×1 elements) analysed using MATLAB.

subject to:

$$\frac{V(x)}{V_0} = f \tag{3}$$

$$\textbf{KU} = \textbf{F} \tag{4}$$

$$0 < x_{min} \leq x_e \leq 1 \tag{5}$$

where, c is total compliance of the structure. 'x' is a vector containing element densities. K is the global stiffness matrix, and U is the global displacement vector. Similarly, xe , ue and k0 are element density, element displacement vector and element stiffness matrix, respectively. N is the total number of elements and the penalty 'p' is a prescribed constant. V(x) is the material volume. V_0 is the total volume of design space, f is the permissible volume fraction and F is the global force vector. The minimum density (xmin) for an element has been taken as 0.001 in accordance with Andreassen et al. (2011). The Method of Moving Asymptotes (MMA) was used for optimization (Svanberg (1987); Sigmund (2007); Prasad and Diaz (2008)).

2.2.2 Minimization of compliance subject to constraint on polar moment of area

This optimization problem is similar to the one in Section 2.2a, however, the weight constraint in (3) is replaced by the constraint on polar moment of area. The constraint can be represented as:

$$a_r(x) \leq a_{r0} \tag{6}$$

where $a_r(x))$ is the sum of first polar moment of area due to individual elements in the design space and $'a_r0')$ is a user defined value. Mathematical expression for $a_r(x))$ is as follows:

$$a_r(x) = \sum_{e=1}^{N} (x_e.|r_e|.a_e) \tag{7}$$

where $a_e$represents area of an element which may be taken as unity and $|r_e|$ is the magnitude of position vector of the element centroid with respect to centroid of the design space.

2.3 Load application scheme

To achieve design space-independency in final results, it is important that loads are not applied at specific points/nodes, as the final design may be biased toward selected loading points. Accordingly, we used a modulus/density dependent loading scheme such that the load is distributed on complete design space rather than select points. The global force vector 'F' in (4) is assembled from individual element force vectors f_e^0 following standard procedure. The distributed of total load (F0) on all elements in the design space is given by:

$$\mathbf{F_e} = \frac{x_e^p \mathbf{F_0}}{\sum_{i=1}^{N} (x_i^p)} \tag{8}$$

The elemental force share $(F_(e))$ is then distributed to the corresponding element nodes. For a typical case of vertical load $'F_0'$ applied only at free end of the beam (i.e. first four nodes are loaded in 2^{nd} degree of freedom direction), the element force vector is computed as follows:

$$\mathbf{f_e^0} = \{0 \quad n_f \quad 0 \quad 0 \quad n_f \quad 0 \quad 0 \quad n_f \quad 0 \quad 0 \quad n_f \quad 0 \quad 0 \quad 0 \quad 0 \quad \cdots 0 \quad 0 \quad \}_{48\times 1} \tag{9}$$

where

$$n_f = \frac{x_e^p.\mathbf{F_0}}{4.\sum_{i=1}^{N} (x_i^p)} \tag{10}$$

A similar scheme was used for torsion application as well. For an externally applied torsional moment $'T_0'$, the elemental force distribution should be such that it maintains constant angular displacement. The elemental share of force should, therefore, be multiplied with distance between element centroid and

Section	Load	Constraint(Specified)
3.1	$\mathbf{F}_{vertical}$	$\mathbf{V_0}^* = 0.5$, $\mathbf{a_{r0}}^* = 1.09e+6$
3.2	Torque	$\mathbf{V_0}^* = 0.5$, $\mathbf{a_{r0}}^* = 1.27e+6$
3.3	$\mathbf{F}_{horizonal}$ and $\mathbf{F}_{vertical}$	$\mathbf{V_0}^* = 0.5$, $\mathbf{a_{r0}}^* = 1.12e+6$
3.4	$\mathbf{F}_{vertical}$+$\mathbf{F}_{axial}$	$\mathbf{V_0}^* = 0.5$, $\mathbf{a_{r0}}^* = 1.9e+5$

* $\mathbf{V_0}$-Volume constraint, * $\mathbf{a_{r0}}$- specified value of polar first moment of area

Table 1: Problem-specific data

torsional axis. Accordingly, an all-new torsion application scheme is derived. The resultant elemental force is given by

$$\mathbf{P_e} = \left[\frac{\mathbf{T}_0}{\sum_{e=1}^{N} (x_e^p)\mathbf{r_e} \times \hat{\theta}_\mathbf{e}\, |\mathbf{r_e}|} \right] x_e^p |\mathbf{r_e}| \hat{\theta_\mathbf{e}} \tag{11}$$

where r_e is the position vector of element centroid with respect to torsional axis and $(\hat{\theta}_\mathbf{e})$ is the unit vector at the centroid of the element in the direction of the force (i.e. inclined 90 degrees with respect to r_e). For a torque $'T_0'$ applied at the free end of a shaft, elemental force vector may be written as:

$$\mathbf{f_e^0} = \{ n_{th} \quad n_{tv} \quad 0 \quad n_{th} \quad n_{tv} \quad 0 \quad n_{th} \quad n_{tv} \quad 0 \quad n_{th} \quad n_{tv} \quad 0 \quad n_{th} \quad n_{tv} \quad 0 \quad \cdots 0 \quad 0 \quad \}_{48\times 1} \tag{12}$$

where n_{th} and n_{tv} are the horizontal and vertical components of nodal force n_t which is one fourth of $\mathbf{P_e}$.

3 Results

The developed methodology is first tested for finding optimal cross-sections in a $3000mm$ long beam having $240 \times 240mm^2$ of square design space (Fig. 2(a-b)) (as in Liu and Jia (2008)). The material is assumed to be isotropic with Young's modulus 'E' of $200GPa$ and Poisson's ratio 'ν' of 0.3 . The design space is discretized using 150×150 (i.e., total 22500) elongated brick elements. The associated data for problems to be discussed in Sections 3.1-3.4 are given in Table 1.

3.1 A single vertical end load

One end of the beam is fixed and a vertical force of 10 kN is applied at the free end (Figs. 2(a,c)). As shown in Figs. 2(d-e), the standard I-section topologies are obtained from both optimization methods, which are also similar to those observed in the literature(Liu et al. (2008); Patel et al. (2009); Yiru et al. (2015)). Despite the similarity, it is worth noticing that, for the same final weight, the I-section obtained through the new method (Fig. 2(e)) seems more robust in terms of thicker web, chamfered web-flange junction and tapered flanges. In addition, the final geometry does not utilize the complete breadth of design space. The aforementioned observations clearly indicate that new method can result in relatively stronger sections in such loading cases.

3.2 Beam section under pure torsion

The beam model used in previous sub-section is used. One end of the beam is fixed whereas a twisting moment of $1.0kNm$ is applied on the free end as shown in Fig. 3(a, c). A hollow circular section similar to that observed in previous studies on shaft optimization is obtained from both the formulations discussed in Sections 2.2a and 2.2b (Figs. 3(d-e)) (Li et al. (2001); Kim and Kim (2000); Ishii and Aomura (2004)). This indicates that the new method is also equally efficient for beam/shaft optimization under torsional loads.

3.3 Bi-axial loading

This is an example of two loading cases, i.e., a beam needs to be designed for two different loading cases similar to that in Ishii and Aomura (2004). Specifically, the cantilever beam is subjected to independent

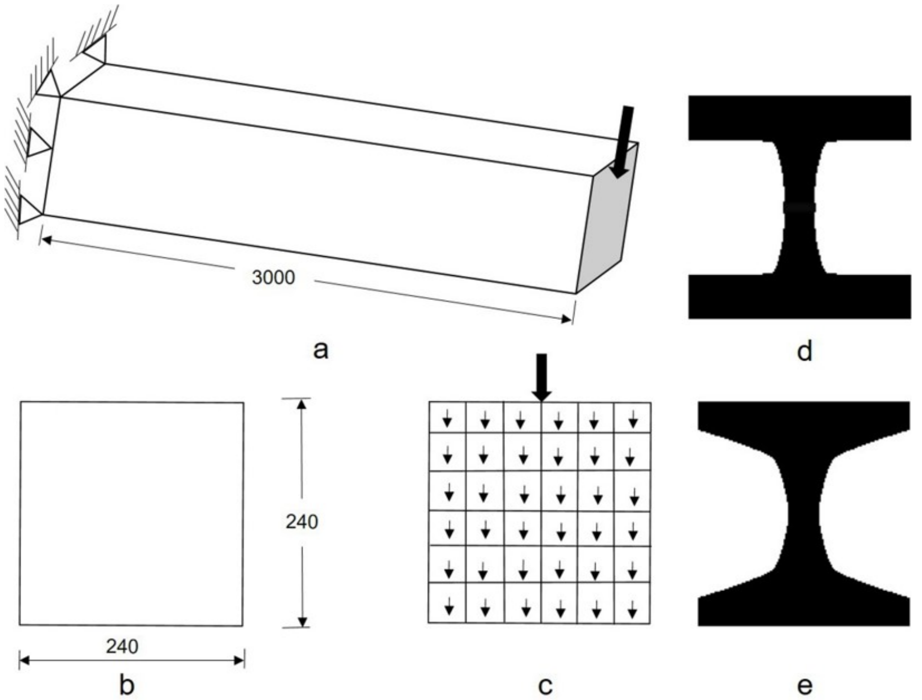

Figure 2: Schematic representation of cantilever beam with a single end load (a), design space dimensions (240mm x 240mm) for designing the beam's cross-section (b), load distribution scheme over the free-end section (c), the optimal section obtained by minimizing compliance subject to the weight constrained to 50% of the design space (d), and the optimal solution obtained by replacing the weight constraint with a constraint on polar first moment of area (e).

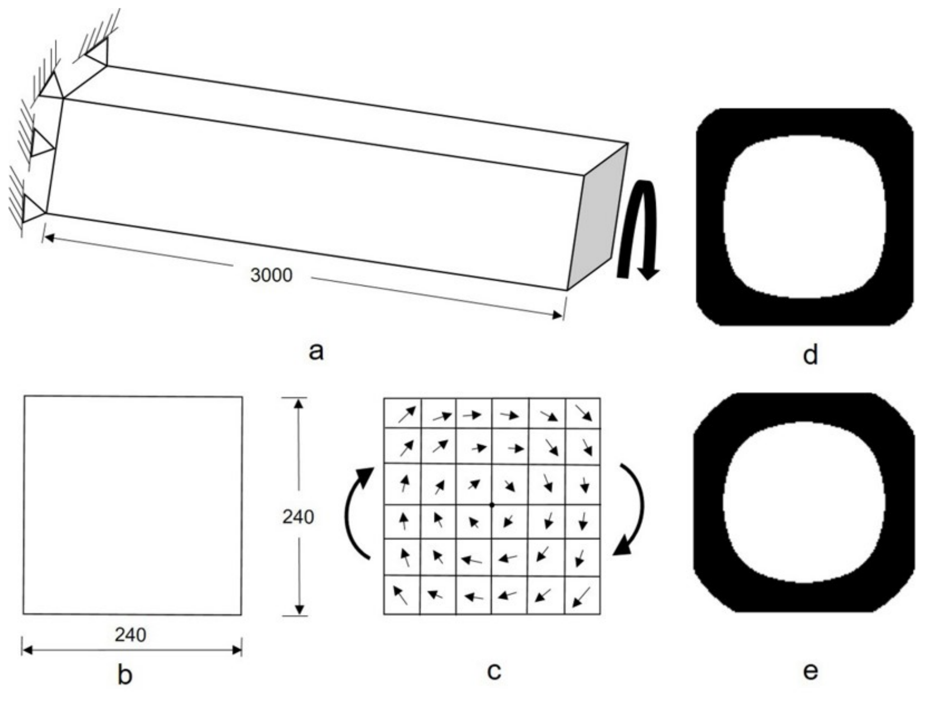

Figure 3: Beam subjected to pure torsion with square section as design space (a-b), load distribution scheme (c), section obtained after minimizing compliance against 50% weight constraint (d) and that after minimization of weight subject to constraint on compliance (e).

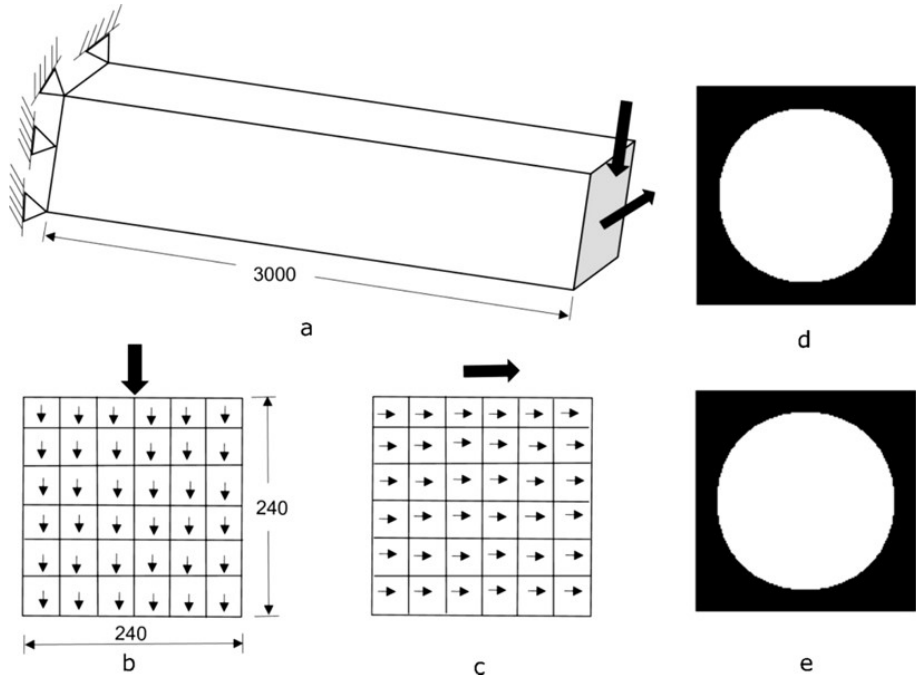

Figure 4: Bi-axial end loading of a cantilever beam (a), load distribution in vertical direction (b), load distribution in horizontal direction (c), outcome of compliance minimization subject to 50% weight constraint when both vertical and horizontal loads have equal magnitude (d), and solution of the corresponding problem with polar moment of area constraint (e).

end loads of $10kN$ in two mutually perpendicular directions (Figs. 4(a-c)). The compliance due to both the loading cases were added and minimized. The result is a square section with a nearly circular cavity, which is also one of the commonly used beam sections (Figs. 4(d-e)). The similarity of results in the two optimization methods indicate that both methods can be used interchangeably in such loading cases.

3.4 Beam subjected to a multi-load case of simultaneous tensile and vertical loading at free end

To test the efficacy of the method with respect to multi-loading conditions and changes in beam/element dimensions, we used a beam of size $100mm \times 100mm \times 1000mm$ which is discretised using the same 16-noded hybrid brick elements. The dimension of each element is $1mm \times 1mm \times 1000mm$ in this case. One end of the beam is fixed while the other end is simultaneously subjected to a vertical load of magnitude 1kN and a tensile load of magnitude 10kN, both distributed over the section. First, the compliance of the beam is minimized for a 50% weight constraint (Fig. 5(a)) which is followed by a constraint on polar first moment of area such that the final weight remains 50% of the design space (Fig. 5(b)). Interestingly, the final topologies are considerably different as the area moment constraint tries to keep the material closer to the centre of the design space. The final compliance values, however, were approximately the same (i.e. 364.72 J and 373.498 J for weight constraint and area moment constraint, respectively). This indicates that both methods are equally efficient in such cases, though the area moment based section seems more appropriate in terms of space utilization, more elegant and robust.

3.5 Demonstrating the ability to generate design space independent beams sections

From the comparison of final topologies in Sections 3.1-3.4, it may be said that the new scheme has a potential to be used as an alternative to the conventional weight constraint-based optimization scheme. However, it is important to notice that in all the cross-sections, most of the material distribution occurs at design space boundaries. This implies that in case a different shape of the design space such as a triangle is used, the final topologies would have been very different from those obtained above. Therefore, in this section, the ability of the new scheme to generate topologies which could have a lower dependence on the shape of design space is demonstrated. This is done by using a considerably low value of constraint on

Figure 5: A cross-section topology obtained for a combination of tensile and vertical loads applied simultaneously at free end of the cantilever beam with 50% weight constraint (a), and the topology with a polar first moment of area constraint such that final weight is approximately 50% of the maximum weight possible for the design space.

polar first moment of area as in order to minimize the compliance, higher allowable values would obviously distribute the material at boundaries. Apart from this, dependence of final shaft topologies on magnitude of the applied torsion is also described.

3.5.1 Bending loads

Single bending load on free end

To demonstrate the design-space-independency feature, two different end-load cases are considered where in the first case, load is applied vertically (similar to that in Section 3.1) and in the second case, load is applied at an angle of 45^0 to the horizontal. The beam models are the same as in Section 3.1 with exception of finite element discretization ($75 \times 75 \times 1$ elements) and load magnitude (7N). Both the beams were first optimized for an area moment constraint value of 5×104 mm3 (Figs. 6(a-b). The final weight fractions were then used to optimize the same beam sections using a weight constraint-based formulation ((Figs. 6(c-d)). As anticipated, the area moment constraint based formulation resulted in approximate H-sections in both the cases whereas the weight constraint based formulation achieved two completely different topologies for change in loading direction (indirectly the shape of design space).

Bi-axial bending

All the beam model parameters are the same as in the bi-axial loading problem discussed in Section 3.3. Five different loading conditions are considered; where in the first case, both vertical and horizontal load has the same magnitude of 500N. In the subsequent cases, the horizontal load is sequentially decreased to zero. All the five cases are run for a fixed value of area moment constraint (i.e., $10^5 mm^3$). Accordingly, the horizontal load is 500N in the first case, 400N in the second, 300N in the third, 100N in fourth, and zero in the last (single load case) (Figs. 7(a-e)). To demonstrate the difference between the outcomes of the two optimization schemes, the first case (i.e., equal bi-axial load) is also solved using conventional weight constraint based formulation for a low constraint value viz. 20% of the maximum possible (Fig. 7(f)). Similar to the single vertical load case, innovative sectional geometries were obtained from the different loading conditions in bi-axial loading too. In particular, the circular and elliptical cross-sections (Figs. 7(a-b)) are difficult to achieve through the conventional method when the beam is subjected to only bending loads. Interestingly, such sections are typically observed in biological tissues such as long bones (Goldman et al. (2009)). Therefore, the introduction of the new scheme could enable the extension of the topology optimization to the area of anatomical research.

3.5.2 Torsion loads

Beam optimization under pure torsion is explored again. The model parameters in this case are adopted from Section 3.2. First, the beam/shaft is optimized for a low value of polar first moment of area constraint (i.e., $10^5 mm^3$) under two different torque magnitudes (i.e., 10^5 Nmm and 5×10^4 Nmm, respectively) (Figs. 8(a-b)). Both problems are then solved using a small weight constraint (i.e., 15% of design space) (Figs. 8(c-d)). It can be observed from Figs. 8(a-b) that the beam under higher torque uses more material than the one with lower torque while maintaining a constant constraint value. However, such difference

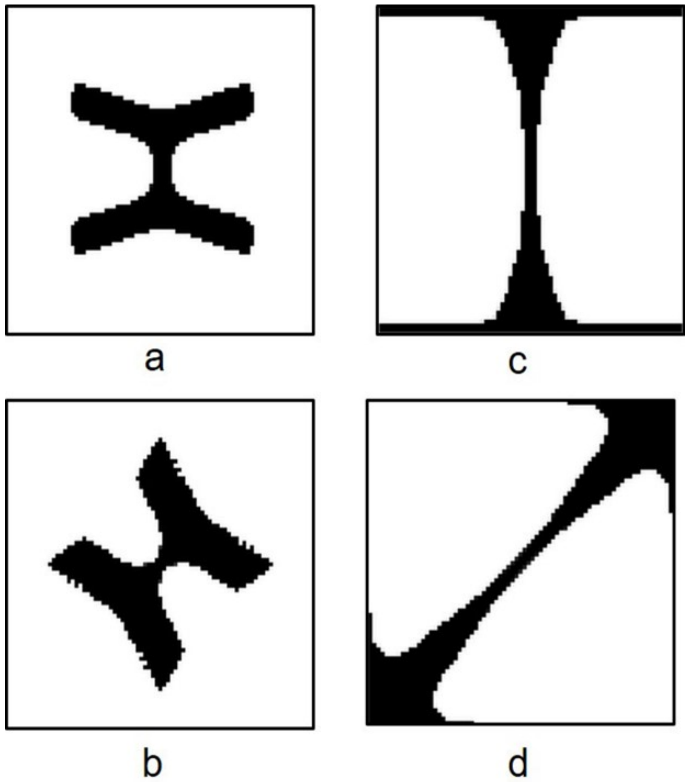

Figure 6: Testing the design-space-independency feature of the new constraint on end-load problems; vertical end-load (a), load at an angle of 45^0 to the horizontal (b), corresponding weight-constraint based topologies (c-d).

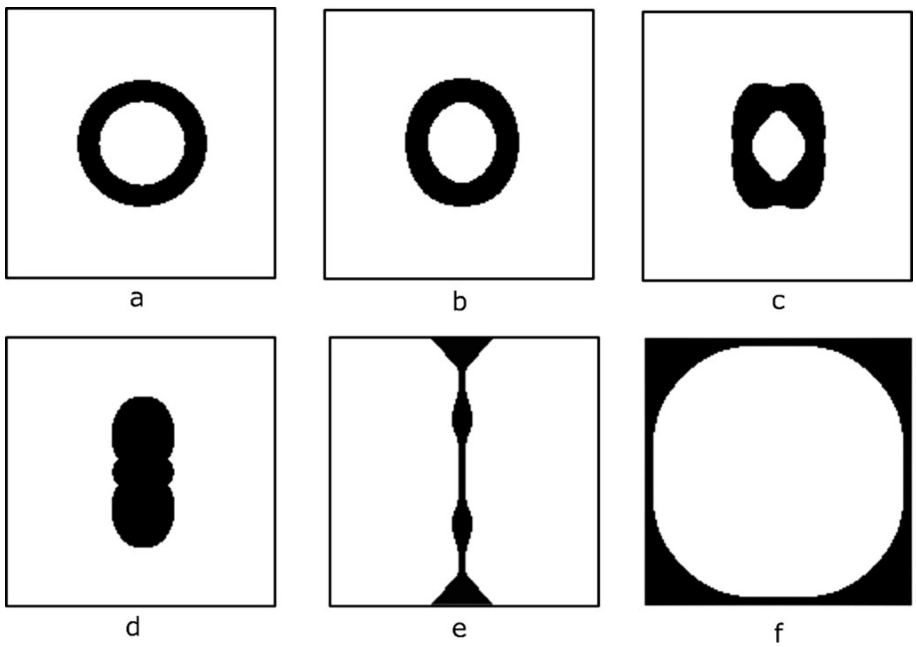

Figure 7: Exploring the design-space-independency feature for varying bi-axial bending loads under a small area moment constraint value; (a) final cross-section for equal bi-axial loads of magnitude 500N, the optimal sections achieved by decreasing the horizontal load magnitude to 400N, 300N and 100N respectively (b-d), geometry with only vertical load applied (e), and the final section obtained using a small weight constraint of 20% with equal bi-axial loads of 500N (f).

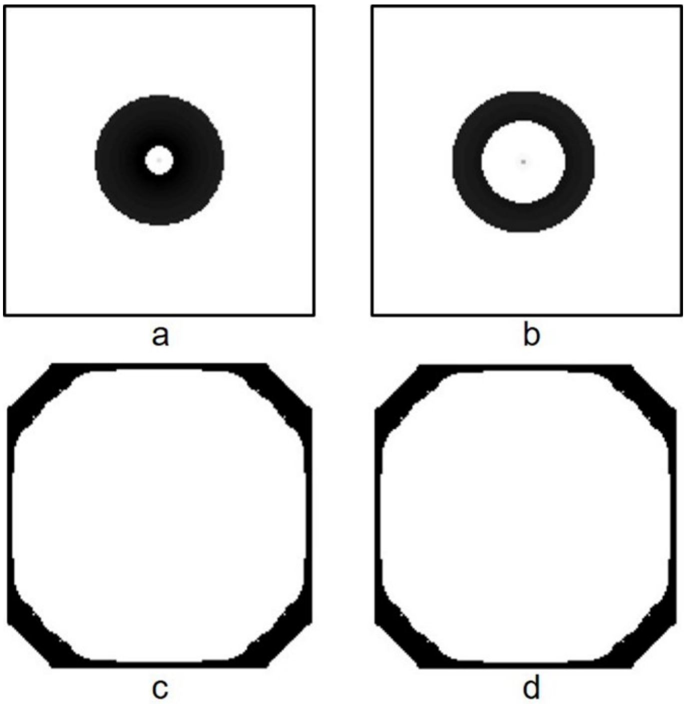

Figure 8: Test of design-space-independency under torsional moment of different magnitudes and small area moment constraint value ($10^5 mm^3$); (a-b) shaft cross-sections with torque magnitudes of 10^5Nmm and 5×10^4 Nmm respectively, and corresponding cross-sections with weight constraints of 15% each (c-d).

is not observed in the corresponding weight-constraint based results (Figs. 8(c-d)) where both geometries are nearly identical. The results present the current scheme as an ideal choice for shaft design as it takes care of all the major design aspects i.e. shape, dimensions and material efficiency.

4 Discussion and Conclusion

A novel method for optimization of beam/shaft cross-sections is presented. In this method, the structural compliance is minimized against a constraint on polar first moment of area (similar to polar moment of inertia) rather than a conventional weight constraint. The constraint is useful as in addition to constraining the weight of the beam, it also constrains the 'enclosed area' of the beam section and thus decreases the dependency on shape of the design space; as can be seen in Figs. 6-8. In addition, the method can suggest compact, realistic and robust I-beam sections having tapered flanges which are typically used in the actual practice (e.g., rail profile). Such compact designs are also expected to have better resistance to lateral (i.e. sectional) buckling (due to a lower lateral slenderness ratio) and twisting/warping (due to thicker/compact size), which are typical concerns during beam design for unforeseen eccentric loading (Liu et al. (2008)). The inherent resistance for warping is an important advantage of this method as most of the existing beam optimization methods did not consider the effect of twisting/warping and lateral buckling (Zuberi et al. (2010); Patel et al. (2009); Ishii and Aomura (2004); Kim and Kim (2000)). Further, the method also introduces and tests a design space-independent loading scheme where the total force or torque is prescribed, which is distributed on the section elements according to their elastic moduli. This scheme along with the polar moment of area constraint can lead to intuitive hollow circular and elliptical sections (Fig. 7) for bi-axial bending cases which has never been achieved using traditional weight/volume/stress/area constraint. Apart from the design-space-independency, the complete formulation (i.e., the objective, constraint, and the loading scheme) also brings in a way to achieve material efficiency in shaft design as both torque and the constraint magnitude govern the final weight of the section (Fig. 8). Further, the dependency of force on elastic modulus of the elements may be particularly suitable for optimizing beam sections composed of multiple materials. The current optimization method may have some limitations as well. Due to its very formulation, the new method may have an inherent affinity towards the centre of design space. Hence, the final topologies obtained through the new method may sometime be inferior to those obtained through conventional weight constrained based method. Therefore, it is advised to use the method as a support rather than a replacement to the conventional method. Similarly, the optimization method may suggest different topologies from a change of parameters due to inherent limitation of gradient based optimization methods (such as the currently used MMA algorithm) to converge to local optima which may sometimes be redundant. Nevertheless, the limitation may be overcome by using global optimization methods (Wang et al. (2001)). Moreover, the new method presents an idea of constraints beyond weight and stress, and is a step towards making design independent of the design space. To summarize, the work is an attempt to overcome the effect of the shape of the design space on topologically optimized beams/shaft sections. The goal is achieved through a new constraint accompanied by a fitting force application method. In addition to design-space-independency, the formulation has an added benefit of achieving material efficiency with respect to the cost of space/radial distance. Complete testing of the formulation was performed using a simplified beam model which is also unique in itself, as it can easily incorporate material anisotropy and inhomogeneity through suitable alteration in element elastic stiffness matrix. Hence, this work has three major contributes to the field of cross-section optimization : (i) the polar first moment of area constraint, (ii) the force and torsion application scheme, and (iii) the simplified model of prismatic beam that can take up realistic loads without requiring an extrusion constraint. Most importantly, all three formulations/contributions are simple enough to be integrated into most of the optimization platforms.

Acknowledgements
Authors acknowledge Department of Science and Technology (Grant No. SB/S3/MMER/0046/2013) for the computational facility. First author also acknowledges IIT Ropar for the institute fellowship.

References

Andreassen, E., Clausen, A., Schevenels, M., Lazarov, B. S., and Sigmund, O. (2011). Efficient topology optimization in matlab using 88 lines of code. *Structural and Multidisciplinary Optimization*, 43(1):1–16, DOI: 10.1007/s00158-010-0594-7.

Bathe, K.-J. (2006). Klaus-Jurgen Bathe, Finite element procedures.

Blasques, J. P. and Stolpe, M. (2012). Multi-material topology optimization of laminated composite beam cross sections. *Composite Structures*, 94(11):3278–89, DOI: 10.1016/j.compstruct.2012.05.002.

Goldman, H. M., McFarlin, S. C., Cooper, D. M., Thomas, C. D., and Clement, J. G. (2009). Ontogenetic patterning of cortical bone microstructure and geometry at the human mid-shaft femur. *Anat Rec (Hoboken)*, 292(1):48–64, DOI: 10.1002/ar.20778.

Ishii, K. and Aomura, S. (2004). Topology optimization for the extruded three dimensional structure with constant cross section. *JSME International Journal Series A Solid Mechanics and Material Engineering*, 47(2):198–206, DOI: 10.1299/jsmea.47.198.

Kim, Y. Y. and Kim, T. S. (2000). Topology optimization of beam cross sections. *International Journal of Solids and Structures*, 37(3):477–93, DOI: http://dx.doi.org/10.1016/S0020-7683(99)00015-3.

Li, Q., Steven, G. P., Querin, O. M., and Xie, Y. M. (2001). Stress based optimization of torsional shafts using an evolutionary procedure. *International Journal of Solids and Structures*, 38(32):5661–77, DOI: http://dx.doi.org/10.1016/S0020-7683(00)00365-6.

Liu, S., An, X., and Jia, H. (2008). Topology optimization of beam cross-section considering warping deformation. *Structural and Multidisciplinary Optimization*, 35(5):403–11, DOI: 10.1007/s00158-007-0138-y.

Patel, N. M., Penninger, C. L., and Renaud, J. E. (2009). Topology synthesis of extrusion-based nonlinear transient designs. *Journal of Mechanical Design*, 131(6):61003–11, DOI: 10.1115/1.3116255.

Popov, E. P. (1968). Introduction to mechanics of solids ".

Prasad, J. and Diaz, A. R. (2008). Viscoelastic material design with negative stiffness components using topology optimization. *Structural and Multidisciplinary Optimization*, 38(6):583–97, DOI: 10.1007/s00158-008-0308-6.

Reddy, J. N. (1993). *An introduction to the finite element method*, volume 2. McGraw-Hill, New York.

Ren, Y., Jinwu, X., Zheqi, L., and Tiantian, Z. (2016). A novel topology optimization method for composite beams. In *Proceedings of the Institution of Mechanical Engineers*, pages 1153–63. Part G: Journal of Aerospace Engineering 230 (7).

Sigmund, O. (2007). Morphology-based black and white filters for topology optimization. *Structural and Multidisciplinary Optimization*, 33(4):401–24, DOI: 10.1007/s00158-006-0087-x.

Svanberg, K. (1987). The method of moving asymptotes—a new method for structural optimization. *International Journal for Numerical Methods in Engineering*, 24(2):359–73, DOI: 10.1002/nme.1620240207.

Vatanabe, S. L., Lippi, T. N., de Lima, C. R., Paulino, G. H., and Silva, E. C. N. (2016). Topology optimization with manufacturing constraints: A unified projection-based approach. *Advances in Engineering Software*, 100:97–112, DOI: 10.1016/j.advengsoft.2016.07.002.

Wang, G., G., Z. D., and Aitchison, P. (2001). Adaptive response surface method - a global optimization scheme for approximation-based design problems. *Engineering Optimization*, 33(6):707–33, DOI: 10.1080/03052150108940940.

Yiru, R., Jinwu, X., and Zheqi, L. (2015). Topology design of composite rotor beam with gradient-based algorithms. *Aircraft Engineering and Aerospace Technology*, 87(4):305–11, DOI: doi:10.1108/AEAT-06-2013-0120.

Zhou, M., Fleury, R., Shyy, Y.-K., Thomas, H., and Brennan, J. (2002). Progress in topology optimization with manufacturing constraints. In of Aeronautics and, A. I., editor, *9th AIAA/ISSMO Symposium on Multidisciplinary Analysis and Optimization*. and Astronautics.

Zuberi, R. H., Zhengxing, Z., Kai, L., and Wen, L. (2010). *Topological optimization of constant beam section under moving load condition*. Paper presented at the Mechanic Automation and Control Engineering (MACE).